THE JOURNAL OF BIOLOGICAL CHEMISTRY
Vol. 271, No. 44, Issue of November 1, pp. 27608–27614, 1996

Printed in U.S.A.

Simultaneous and Different Binding Mechanisms of 4′,6-Diamidino-2-phenylindole to DNA Hexamer $(d(CGATCG))_2$

A ^{1}H NMR STUDY*

(Received for publication, June 19, 1996, and in revised form, August 13, 1996)

Edoardo Trotta‡§, Ettore D'Ambrosio‡, Giampietro Ravagnan‡, and Maurizio Paci¶

From the ‡Consiglio Nazionale Ricerche, Istituto di Medicina Sperimentale, Viale Marx 15, I-00137 Rome and the §Dipartimento di Scienze e Tecnologie Chimiche, Universita' di Roma "Tor Vergata," I-00133 Rome, Italy

The solution structure of the complex between 4′,6-diamidino-2-phenylindole (DAPI) and DNA oligomer $(d(CGATCG))_2$ at a 2:1 drug/duplex ratio has been characterized by combined use of proton one- and two-dimensional NMR spectroscopy, molecular mechanics, and molecular dynamics computations. Intermolecular nuclear Overhauser effects (NOEs), DNA structure perturbations, and resonance shifts induced by binding provide evidence that DAPI interacts with DNA hexamer by two different binding mechanisms, in fast exchange on the NMR time scale, without any significant distortion of the B-type conformation of DNA hexamer. The results indicate that the ligand binds into the minor groove of the central 5′–ATC-3′ region of the hexamer and on the outside of the oligomer by a π,π-stacking interaction with the terminal C1:G6 base pairs. A model for both binding mechanisms that accounts for all experimental data was generated by molecular mechanics and dynamics calculations based on experimental NOEs. In the minor groove binding, N2 amino group of G2 precludes a deep insertion of phenyl ring of DAPI into the groove. Position and orientation of the drug in the external stacking interaction resemble those suggested for intercalation of DAPI between C:G base pairs.

A number of DNA-binding drugs modulate the activity of enzymes involved in the DNA metabolism by interfering with the access of DNA-binding proteins to specific DNA sequences. Therefore, a detailed characterization of the molecular aspects of ligand-DNA recognition appears essential for helping in planning new drugs with clinically appreciable effects and for elucidating the processes that regulate gene expression in the cells.

It is shown that synthetic antibiotic 4′,6-diamidino-2-phenylindole (DAPI)[1] (Fig. 1) interferes with the activity of some DNA processing enzymes involved in regulatory and structural functions (1–7). Strong inhibitory activity of this drug has been reported for RNA polymerase II and attributed to its high affinity binding in the minor groove of AT sequences (7). Such a strong DAPI-DNA interaction interferes with the binding of TBP (TATA-binding protein) to its consensus TATA box sequence, preventing the formation of the transcription factors-DNA complex recognized and required by RNA polymerase II for initiating gene transcription. It has been also reported that DAPI is active on other DNA-directed enzymes such as DNA ligase, exonuclease III, and DNA polymerase I showing varying levels of inhibitory activity (5). Such a differential action of DAPI appears not simply attributable to its AT-specific minor groove binding, as invoked in the case of RNA polymerase II. For attempting to explain the biological effects of the drug, deeper insight into the structural aspects of DAPI·DNA complexes appears necessary.

The DAPI complexes with natural and synthetic DNA have been the object of several studies evidencing the complexity and heterogeneity of the interaction that appears strongly dependent on the DNA sequence and on the ligand-nucleotide binding ratio (8–23). In spite of new reports in the literature in the last few years, these two aspects of the binding are still not well understood. It is well established that both the affinity and the geometry of the binding of DAPI is strongly dependent on the DNA sequence. DAPI preferentially binds DNA in the minor groove of sequences containing two or more contiguous A:T base pairs. However, at high binding ratios, optical spectroscopy studies evidenced two different bound ligands in complexes of DAPI with short oligomers containing one minor groove binding site (24). Moreover, minor groove binding to more than one AT-rich site appears heterogeneous and exhibits positive cooperativity (8, 21, 24). It has been also reported that DAPI binds DNA sequences containing no contiguous A:T base pairs. This binding mode appears very different from the minor groove interaction, and both intercalation and major groove interaction have been proposed (8–10, 16). Recently, experimental evidences by ^{1}H NMR spectroscopy have been reported that support a mechanism of interaction of DAPI with 5′-CG-3′ sites by intercalative binding (20).

In the present paper we report an NMR study of DAPI bound to a short DNA oligomer $(d(CGATCG))_2$ at high molar ratios for investigating its distinct binding mechanisms and their compatibility inside short DNA sequences. The results provide evidence that DAPI interacts with the DNA oligomer by at least two simultaneous and different binding mechanisms. In addition to the minor groove interaction, a new binding involving an external stacking interaction of the drug with the terminal base pairs of the oligomer is proposed.

EXPERIMENTAL PROCEDURES

Sample Preparation—The DNA oligomers were synthesized by an Applied Biosystems 391 instrument on a 10-μmol scale and purified, after deprotection, as described previously (20). DAPI was purchased from Sigma and used without further purification. The purity of DAPI and DNA oligomers was checked by ^{1}H NMR, and concentration was measured spectrophotometrically using ϵ_{255} (KOH 0.1 M) = 57,000 (25) and ϵ_{342} = 23,000 M^{-1} cm^{-1} (26), respectively. NMR samples were

* The costs of publication of this article were defrayed in part by the payment of page charges. This article must therefore be hereby marked "*advertisement*" in accordance with 18 U.S.C. Section 1734 solely to indicate this fact.

¶ To whom correspondence should be addressed. Fax: 39-6-86090332; E-mail: edoardo@biocell.irmkant.rm.cnr.it.

[1] The abbreviations used are: DAPI, 4′,6-diamidino-2-phenylindole; DQF, double-quantum filtered; COSY, correlated spectroscopy; NOE, nuclear Overhauser effect; NOESY, NOE spectroscopy; TOCSY, total correlated spectroscopy.

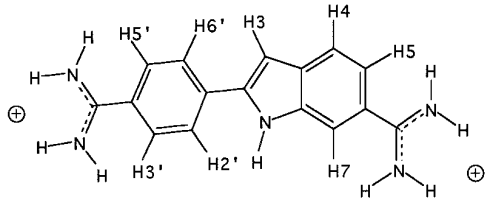

FIG. 1. **Chemical structure and proton numbering of DAPI.**

suspended in 50 mM NaCl, 10 mM sodium phosphate at pH 7.00, in 100% D_2O or 90% H_2O and 10% D_2O for H_2O solutions. Saturating concentration of DAPI in the buffer of NMR samples was 26 μM, as measured spectrophotometrically in the absence of DNA. The concentrations of DAPI and $(d(CGATCG))_2$ in the 2:1 drug/duplex solution were 4 and 2 mM, respectively.

NMR Spectroscopy—NMR spectra were obtained using a Bruker AM 400 and a Bruker AMX 600 instruments operating at 400 and 600 MHz, respectively. D_2O and H_2O one-dimensional NMR spectra were run over about 10 and 20 ppm spectral width, respectively, and accumulated on 16K or 32K of memory with carrier frequency centered on water resonance. The ppm scale was referenced to tetramethylsilane, assuming residual protonated water HDO as 4.76 ppm.

Correlation two-dimensional NMR spectra were performed by using double quantum filtered COSY (27), primitive exclusive COSY (28), and TOCSY with a MLEV-17 pulse sequence to substitute the spin-lock period (29, 30). Two-dimensional exchange spectroscopy was performed by NOESY experiments (31) at mixing times ranging from 50 to 300 ms. Two-dimensional NMR spectra were typically run recording from 300 to 700 experiments over 2K of memory in phase-sensitive mode using time-proportional phase incrementation (32). A recycle delay of 2.2 s was used. π/3-shifted sine-bell or π/2-shifted squared sine-bell window functions were applied in both directions. Suppression of water signal in one- and two-dimensional spectra of H_2O samples was obtained with 1–1 spin echo pulse sequence 90_x-t-90_{-x} -D-90_ϕ-2t-$90_{-\phi}$-D-AQ (33). To optimize the solvent suppression and the excitation profile of the 1–1 echo sequence, a short homospoil (1.5–10 ms) was applied during the mixing time; the carrier frequency was adjusted to the water resonance, D = 50 μs, and t = 220 or 85 μs were used for DNA alone or complexes, respectively.

All data were processed on a Digital VaxStation 3100 graphic terminal using the Triton NMR software of the NMR Group of the Department of the Organic Chemistry, University of Utrecht, The Netherlands (34).

Molecular Modeling—Molecular modeling and calculations were carried out using InsightII version 2.3.0 and Discover version 2.9.5 software packages (Biosym Technologies, Inc) on a Silicon Graphics workstation. AMBER force field was employed in all calculations, and previously reported partial atomic charges for DAPI were used (18). Calculations were performed *in vacuo*, and a distance-dependent dielectric constant $\epsilon = r_{ij}$ and $\epsilon = 4r_{ij}$ was used to simulate solvent effects in molecular mechanics and dynamics calculations, respectively. A cutoff of 18 Å with a switching distance of 2 Å was used for non-bonded interactions and 1,4 electrostatic interactions were scaled by 0.5. The initial structures were firstly subjected to NOE-restrained energy minimization with 100 cycles of steepest descents method and 3000 cycles of conjugated gradient minimization. The energy-minimized structures were then subjected to NOE-restrained Verlet molecular dynamics by heating to 300 K during 2 ps followed by 10 ps of constant temperature simulation with time steps of 0.5 fs. Finally, the average structure of the last 1-ps molecular dynamics simulation were further refined by restrained energy minimization until the maximum derivative was less then 0.5 kcal mol^{-1} $Å^{-1}$ followed by 500 cycles of unrestrained energy minimization. DNA NOE-derived distances involving base-base and base-H1′ protons were referenced to cytosine H5-H6 distance (2.45 Å). All the remaining intramolecular DNA distances involving deoxyribose-deoxyribose and deoxyribose-base protons were referenced to H1′-H2″ distances (2.35 Å) of the respective residue (35). Intramolecular DNA distances were calculated from cross-peak volumes of NOESY spectra acquired with 50- and 100-ms mixing times by the isolated spin-pair approximation relationship $r_{ij} = r_{ref}(NOE_{ref}/NOE_{ij})^{1/6}$ where r_{ij} and NOE_{ij} are unknown distance and measured NOE volume between protons i and j, and r_{ref} and NOE_{ref} represent the reference distance and the relevant NOE volume. Lower and upper bounds of distances in restrained calculations were set ±0.5 and 0.8 Å around calculated distance for 50 and 100 ms mixing time NOESY experiments, respectively. DAPI-DNA intermolecular distance restraints were not evaluated from intramolecular reference distances since fast exchange of ligand between different binding sites should cause overestimation of intermolecular distances, depending on the time of residence of the drug in the site of interaction. For this reason all lower bounds for intermolecular distances were set to 1.7 Å and upper bounds up to 2.5, 3.5, and 4.5 Å depending on NOE intensities classified into weak, medium, and strong, respectively.

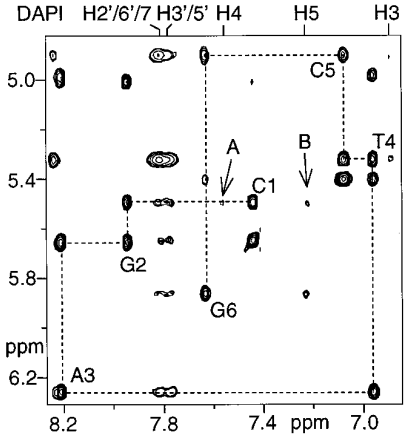

FIG. 2. **Expanded region of NOESY spectrum of a 2:1 DAPI·$(d(CGATCG))_2$ complex acquired with a mixing time of 300 ms, in a D_2O buffer, at 25 °C.** The *broken line* indicates the sequential assignment via H6/H8-H1′ with intranucleotide cross-peaks labeled. The *arrows* indicate the intermolecular NOEs: DAPIH4-C1H1′ (*A*) and DAPIH5-C1H1′ (*B*).

RESULTS AND DISCUSSION

Proton Resonance Assignments and DNA Structure—The proton resonances of free DNA were assigned by COSY, TOCSY, and NOESY experiments by following the standard procedures described in the literature (36–42). The conformation of free $(d(CGATCG))_2$ was evaluated from the intensities of NOESY cross-peaks in experiments acquired with short mixing time (70 ms) and from the values of vicinal coupling constants measured in one-dimensional and primitive exclusive COSY spectra (43–47). The results are consistent with a predominant B-type conformation in agreement with a previously reported study (48).

The assignment of DNA resonances in the complex was performed by applying the same procedures used for DNA alone and verified by a direct comparison with the original DNA spectrum in titration experiments. Fig. 2 shows the sequential assignment of DNA resonances in the complex using NOEs between base H6/8 and deoxyribose H1′ protons. The assignment of the proton resonances of $(d(CGATCG))_2$ in the free form and in the complex is reported in Table I.

Following the same procedure already described (19, 20), the DAPI resonances in the complex at 7.83, 7.80, 7.58, 7.25, and 6.91 ppm were assigned to H2′/6′/7, H3′/5′, H4, H5, and H3 protons, respectively.

Comparison of NOESY spectra acquired with 50-ms mixing time does not reveal significant alteration of B-like structure of DNA upon binding with DAPI. DNA conformation in the complex appear homogeneous along the whole sequence, and the presence of interstrand NOEs between guanine H1 and cytosine H4 as well as thymine H3 and adenine H2 protons shows that base pairing is conserved also at a 2:1 drug/duplex molar ratio. Intranucleotide NOE-derived distances d_i(H6/8 − H1′) >3.5 Å for all purine and pyrimidine residues, according with *anti* conformation of glycosidic torsion angle $\chi \approx -115 \pm 30°$ of B-DNA, rule out the presence of left-handed Z-DNA conformations. This is confirmed by the observed relative intensities of NOEs between H6/H8 and H2′/H2″ protons that are characteristic of B-type DNA structures: H2′(i)-H6/8(i) > H2″(i)-H6/8(i +

TABLE I
Proton chemical shift values (ppm) of (d(CGATCG))$_2$

Base	H1′	H2′	H2″	H3′	H4′	H5′.5″	H6/8	H2/5/Me	H1/3	H4(1)	H4(2)
						free DNA					
C1	5.80	1.90	2.42	4.73	4.10	3.75	7.64	5.93		8.32	6.97
G2	5.62	2.78	2.86	5.05	4.38	4.02, 4.13	8.02		12.92		
A3	6.37	2.76	3.01	5.09	4.54	4.28	8.33	7.99			
T4	6.02	2.07	2.48	4.90	4.24	4.35	7.26	1.47	13.73		
C5	5.84	2.05	2.42	4.88	4.18	4.12	7.53	5.74		8.63	7.06
G6	6.21	2.67	2.44	4.73	4.23	4.13	7.99		13.17		
						2:1 DAPI-duplex complex					
C1	5.53	1.67	2.30	4.66	4.06	3.76	7.46	5.68		8.17	6.78
G2	5.68	2.75	2.88	5.03	4.38	4.11, 4.02	7.96		12.73		
A3	6.28	2.65	2.87	5.01	4.45	4.26	8.23	8.26			
T4	5.34	1.74	2.01	4.54	2.78	3.91	6.98	1.33	14.01		
C5	4.92	1.58	1.92	4.50	2.77	3.68, 3.19	7.09	5.43		8.38	6.78
G6	5.89	2.47	2.19	4.61	4.02	3.60, 4.00	7.65		12.62		

1) > H2′(i)-H6/8(i + 1). Furanose ring conformation was evaluated lying in the south conformation range of B-DNA by the relative intranucleotide NOE intensities H4′-H3′ > H4′-H1′ > H4′-H2″. In addition, no increasing of internucleotide sequential distances were observed upon binding.

Chemical Shift Changes upon Binding—CG-type intercalation and AT-selective minor groove bindings of DAPI induce very different and characteristic shifts of the DNA imino proton resonances. Therefore, titration experiments were performed by following the spectral changes of the imino resonances upon addition of small volumes of concentrated drug solution to the DNA sample.

Imino proton resonances of hexamer continuously shift upon titration, and no new resonances appear in the spectra indicating that free and bound species are in fast exchange on the NMR time scale also at temperature of 6 °C (Fig. 3). At a drug/duplex ratio of 2:1, the imino resonance H3 of T4 is 0.28 ppm downfield shifted while the imino resonances H1 of G2 and G6 are 0.19 and 0.55 ppm upfield shifted, respectively.

Nonexchangeable proton resonances of (d(CGATCG))$_2$ exhibit upfield or no shift except A3H2 resonance which is 0.27 ppm downfield shifted at 2:1 drug/duplex ratio. The strongest chemical shift perturbations of DNA resonances are observed for protons belonging to T4 and C5 residues and exposed in the minor groove. In particular, H1′T4, H4′T4, H1′C5, and H4′C5 resonances exhibit the largest upfield shifts of 0.68, 1.46, 0.92 and 1.41 ppm, respectively. In Fig. 4 the chemical shift perturbations induced by DAPI on the DNA hexamer are plotted *versus* the DNA sequence and compared with those observed in the minor groove complex previously reported (19). As shown, DAPI induces quite similar effects in the central region of the two oligomers, whereas the H1′, H2′, H2″, and H6/8 resonances of C1 and G6 of (d(CGATCG))$_2$ appear clearly upfield shifted in comparison with the resonances of G1, C2, G7, and C8 of the octamer. Moreover, it has been previously reported that minor groove binding to contiguous A:T base pairs induces slight downfield shift of non-exchangeable DAPI resonances, whereas strong upfield shifts were observed in complex of the drug with mixed and C:G sequences and attributed to an effect of intercalation binding mechanism. In this work, DAPI resonances shift 0.2–0.3 ppm upfield upon binding, less than induced by intercalation binding of the ligand to (d(CGACGTCG))$_2$ (0.4–0.7 ppm) previously reported (20).

Intermolecular NOEs in the DAPI·[d(CGATCG)]$_2$ Complex—NOESY spectra of the DAPI·[d(CGATCG)]$_2$ complex at a molar ratio of 2:1 exhibit several dipolar contacts between drug and DNA protons. Figs. 5 and 6 show the regions of a NOESY spectrum of the complex, acquired with a mixing time of 100 ms, which contain the intermolecular cross-peaks of nonexchangeable proton resonances. The spectrum exhibits 20 intermolecular cross-peaks, 14 of which are between ligand protons and minor groove protons of the internal 5′-ATC-3′ region. The only intermolecular NOE contacts involving DNA protons lying in the major groove of double helix are observed with G6H8 and C1H5. In addition, a long mixing time (300 ms) NOESY experiment acquired in D_2O solution was analyzed (Fig. 2). Some useful structural information can be deduced from this spectrum, despite the presence of strong spin diffusion effects. As shown in Fig. 2, H1′ proton of C1 residue exhibits weak dipolar contacts with H4 as well as H5 but not with H3 drug proton. Since no intermolecular NOEs are observed involving G2 protons, these contacts are not attributable to spin diffusion through the adjacent nucleotide as well as H3 proton of DAPI and should be considered in the molecular modeling of binding. This is also true for the dipolar contact (not shown) observed between DNA C1H6 and DAPI H5. It should also be noted that in the long mixing time-acquired spectra, no intermolecular NOEs are observed involving exocyclic methyl protons of thymines exposed in the major groove. In addition, NOESY spectra, acquired in H_2O solution at 6 °C with a mixing time of 250

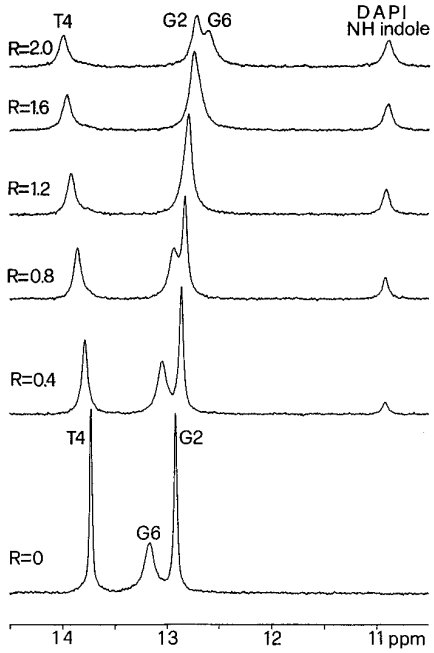

FIG. 3. **Imino proton spectra of DAPI·(d(CGATCG))$_2$ complexes as a function of increasing concentration of DAPI.** The spectra were acquired at 6 °C, with a 1–1 spin echo pulse sequence to suppress water signal. *R* indicates drug-duplex molar ratio.

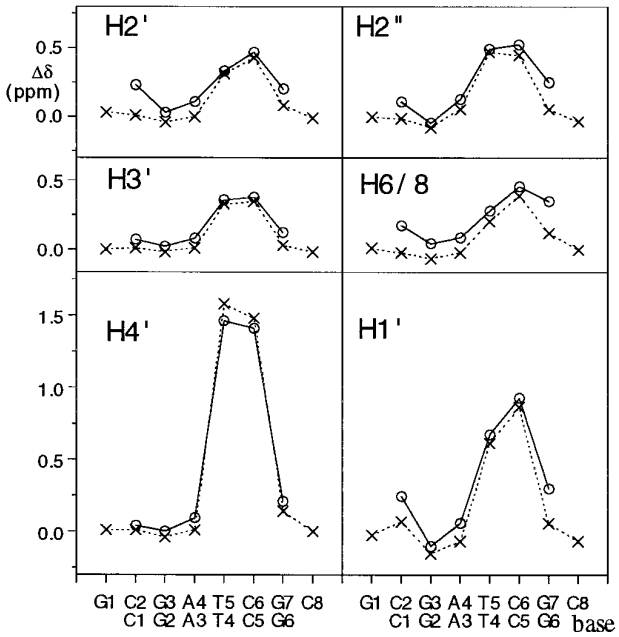

FIG. 4. **Chemical shift changes ($(\Delta\delta = \delta_{free} - \delta_{bound})$ plotted *versus* their position in the sequence.** Resonances belonging to the 1:1 DAPI·(d(GCGATCGC))$_2$ and the 2:1 DAPI·(d(CGATCG))$_2$ complexes are marked by (×) and (○), respectively.

ms, exhibit further intermolecular NOEs involving exchangeable protons. NH indole resonance of DAPI shows NOEs with A3H2 and an unresolved H4′/H5′ DNA resonance; moreover DNA G2H1 and T4H3 exhibit dipolar contacts with DAPI resonances belonging to H7 and phenyl ring.

Binding Mechanisms—Saturating concentration of DAPI in the buffer used for our NMR samples (about 26 μM) is very low in comparison with the total concentration of added ligand in the 2:1 drug-duplex complex (4 mM). For this reason, at least two sites of binding of DAPI to hexamer have to be considered in the molecular modeling of the interaction.

Very different perturbations of the proton chemical shifts of DAPI and DNA resonances have been described in the literature for the CG-type intercalation and the AT-specific minor groove binding (10, 19, 20). In the present study characteristic results of the two binding mechanisms were observed in separated regions of the DNA hexamer. In the central 5′-ATC-3′ region DAPI binding induces the spectral changes described for the minor groove interaction of the drug with (d(GCGATCGC))$_2$ previously reported (19). Downfield shift of thymine H3 and adenine H2 resonances as well as all the strong upfield shifts of DNA proton resonances are observed (Figs. 3 and 4). Intermolecular NOEs are also consistent with the previously characterized minor groove complexes. Considering the central 5′-GATC-3′ DNA region, intermolecular dipolar contacts were observed only with protons exposed in the minor groove. Moreover, as reported in the previous NMR study of DAPI bound into the minor groove of 5′-GATC-3′ (19), the NH indole proton of the ligand exhibits a dipolar contact with adenine H2, and the strongest intermolecular NOEs are observed between the phenyl protons of the drug and adenine H2 and thymine H1′ protons of DNA. In addition, the NOE data show a good qualitatively agreement with the crystal structure of the minor groove complex previously reported (13). This strong correlation between our results and the previous structural studies of DAPI·DNA complexes supports a mechanism of binding of the drug in the minor groove of the central region of our hexamer with its NH indole proton located between the two O2 of the central thymines and oriented toward the DNA helix axis.

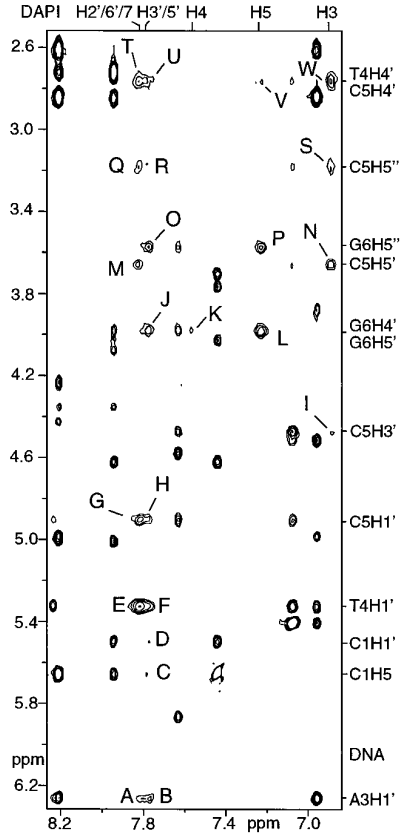

FIG. 5. **Expanded region of NOESY spectrum of a 2:1 DAPI·(d(CGATCG))$_2$ complex acquired with a mixing time of 100 ms, in a D_2O buffer, at 25 °C.** Intermolecular DAPI-DNA cross-peaks are labeled and assigned as follow: *A*, H2′/6′/7-A3H1′; *B*, H3′/5′-A3H1′; *C*, H3′/5′-C1H5; *D*, H3′/5′-C1H1′; *E*, H2′/6′/7-T4H1′; *F*, H3′/5′-T4H1′; *G*, H2′/6′/7-C5H1′; *H*, H3′/5′-C5H1′; *I*, H3-C5H3′; *J*, H3′/5′-G6H4′/5′; *K*, H4-G6H4′/5′; *L*, H5-G6H4′/5′; *M*, H2′/6′/7-C5H5′; *N*, H3-C5H5′; *O*, H3′/5′-G6H5″; *P*, H5-G6H5″; *Q*, H2′/6′/7-C5H5″; *R*, H3′/5′-C5H5″; *S*, H3-C5H5″; *T*, H2′/6′/7-T4/C5H4′; *U*, H3′/5′-T4/C5H4′; *V*, H5-T4/C5H4′; *W*, H3-T4/C5H4′.

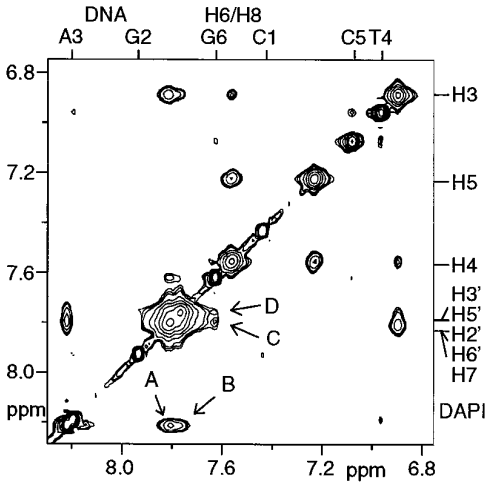

FIG. 6. **Expanded region of NOESY spectrum of a 2:1 DAPI·(d(CGATCG))$_2$ complex acquired with a mixing time of 100 ms, in a D_2O buffer, at 25 °C.** The *arrows* indicate intermolecular DAPI-DNA cross-peaks as follow: *A*, H2′/6′/7-A3H2; *B*, H3′/5′-A3H2; *C*, H2′/6′/7-G6H8; *D*, H3′/5′-G6H8.

As far as the extremities of the hexamer are concerned, the results are not in line with a only minor groove complex suggesting the presence of a second site of binding that involves the C:G ends of the oligomer. In contrast to the previous NMR-characterized minor groove complex, the resonances of DNA

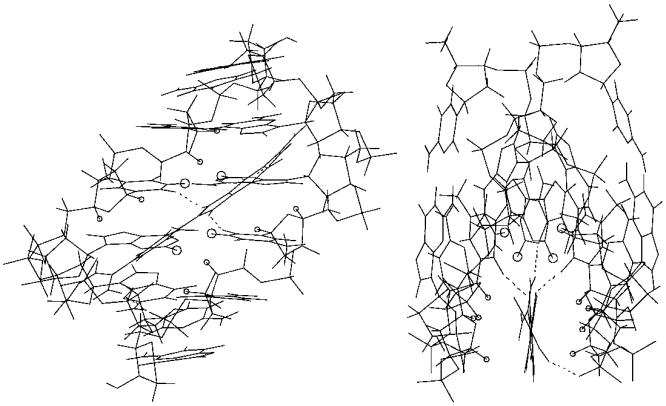

FIG. 7. **Model of the minor groove complex DAPI·(d(CGATCG))$_2$, obtained after molecular mechanics and dynamics calculations.** Views looking into the minor groove normal to the helix axis (*left*) and from end of oligomer (*right*). *Open circles* indicate the DNA protons of 5′-GATC-3′ region that exhibits the strongest upfield (*small circles*) and downfield (*large circles*) shifts of their resonances upon binding.

protons located outside the minor groove binding site appear perturbed (Figs. 3 and 4). Particularly significant is the strong upfield shift of G1 imino resonance (0.55 ppm) which was previously observed in the CG-type DAPI·intercalated complexes (10, 20) and generally considered as a characteristic result of intercalator-induced ring current effects (49). This result suggests a π,π-stacking interaction of DAPI with the last C:G base pairs confirmed by the observed intermolecular NOEs involving DNA protons belonging to both minor and major groove of C1 and G6 residues.

For this reason molecular modeling of the interaction was first performed on minor groove complex using intermolecular NOE-derived distances concerning only A3, T4, and C5 residues. Afterwards, based on minor groove binding model, not compatible intermolecular NOEs were used as a starting point for building a second binding model accordingly with DNA structure and chemical shift perturbations observed.

Molecular Modeling of Minor Groove Complex—Coordinates of the starting model for molecular mechanics and molecular dynamics calculations were taken from the crystal structure of the minor groove complex of DAPI with (d(CGCGAATTCGCG))$_2$, previously reported, after appropriate modifications to obtain our oligomer length and base sequence. The qualitatively good agreement between crystal structure and our intermolecular NOE-derived distances helped us to assign distance restraints to the NMR-equivalent strands of DNA hexamer. Fig. 7 shows two different views of the final refined structure of the minor groove complex obtained as reported under "Experimental Procedures" by using intermolecular NOE-derived distance restraints involving only the internal 5′-GATC-3′. The last structure refinement of the complex by unrestrained molecular mechanics calculations did not result in any significant conformational change indicating that minimum of energy is well reached by calculations. As shown in Table II, all short intermolecular proton distances measured in the refined structure are consistent with the observed intermolecular NOEs involving the internal 5′-GATC-3′ region of hexamer. As a result of the short lifetime of the complex, which causes a decrease in the effective time of intermolecular contacts with respect to the nominal mixing time of NOESY experiments, all intermolecular NOEs appear slightly weaker in comparison with intramolecular NOEs. The refined structure is also consistent with the observed strong perturbations of DNA resonances induced by binding in the internal 5′-GATC-3′ region and not attributable to an alteration of hexamer structure which conserves its B-type conformation. As evidenced in Fig. 7, the position and orientation of aromatic rings of DAPI in the model are consistent with the large upfield shift of H1′ and H4′ resonances of T4 and C5 residues as well as the large downfield shift of A3H2 and T4H3 resonances. In the model DAPI molecule is located nearly isohelical with its NH indole proton oriented toward DNA helix axis and forming a bifurcated hydrogen bond with the two O2 groups of thymine. The structure is further stabilized by hydrogen bonds between indole amidine group of ligand and A3N3 as well as phenyl amidine and O1P of G6 residue. Indole group of DAPI is more deeply inserted into the minor groove than phenyl ring making more favorable van der Waals interaction with DNA double helix. Steric clash and electrostatic repulsion due to N2 amino group of G2 push phenyl amidine toward periphery of the minor groove. This prevents any formation of hydrogen bonds between phenyl amidine and DNA bases.

TABLE II
Intensities of observed intermolecular NOEs and intermolecular proton short distances (<4 Å) involving the internal 5′-GATC-3′ region of DNA hexamer

NOE intensities were measured in a NOESY spectrum of the 2:1 DAPI-(d(CGATCG))$_2$ complex acquired with a 50-ms mixing time; intermolecular distances were obtained from the NMR-refined structure of the minor groove complex.

Intermolecular NOEs		Intermolecular distances[a]	
DAPI-DNA	Intensity[b]	DAPI-DNA	Distance
			Å
H2′/6′/7-A3H2	s	H7-A3H2(+)	2.16
		H6′-A3H2(−)	2.23
H2′/6′/7-T4H1′	s	H6′-T4H1′(−)	2.75
		H7-T4H1′(+)	2.95
H3-T4H4′/C5H4′	m	H3-C5H4′(+)	2.83
		H3-C5H4′(−)	3.10
H2′/6′/7-T4H4′/C5H4′	m	H2′-C5H4′(+)	2.95
		H6′-C5H4′(+)	3.81
		H7-T4H4′(+)	3.85
H2′/6′/7-C5H5′/5″	m	H2′-C5H5′(−)	3.11
		H2′-C5H5″(−)	3.74
H3′/5′-A3H2	m	H5′-A3H2(−)	3.13
H2′/6′/7-C5H1′	m	H6′-C5H1′(+)	3.18
		H7-C5H1′(−)	3.43
H3-C5H5′/5″	m	H3-C5H5′(+)	3.21
		H3-C5H5′(−)	3.54
		H3-C5H5″(+)	3.63
		H3-C5H5″(−)	3.94
H3′/5′-C5H1′	w	H5′-C5H1′(+)	3.26
H3′/5′-A3H1′	w	H5′-A3H1′(−)	3.36
H4-T4H4′/C5H4′	w	H4-C5H4′(−)	3.36
H5-T4H4′/C5H4′	w	H5-T4H4′(+)	3.37
H3′/5′-T4H1′	w	H5′-T4H1′(−)	3.43
H3′/5′-T4H4′/C5H4′	w	H5′-T4H4′(−)	3.50
		H3′-T4H4′(−)	3.94

[a] + and − indicate the two DNA strands.
[b] w, m, and s represent a classification of NOE intensity into weak, medium, and strong, respectively.

As far as the external C1:G6 base pair is concerned, NOEs between drug protons and H4′, H5′, and H5″ protons of G6 appear consistent with the minor groove interaction and can be attributed to this binding. In contrast, long interproton distances in the model are measured for the observed intermolecular NOEs: DAPIH3′/H5′-G6H8 (8.37/6.57 Å), DAPIH2′/6′/7-G6H8 (8.75/6.91/6.47 Å), DAPIH3′/H5′-C1H1′ (16.10/11.88 Å), DAPIH3′/H5′-C1H5 (15.94/11.91 Å), DAPIH4-C1H1′ (16.26 Å), DAPIH5-C1H1′ and DAPIH5-C1H6 (15.80 Å) (Figs. 2, 5, and 6).

Molecular Modeling of Stacking Interaction—The comparative analysis of DNA chemical shift perturbations induced by DAPI in the 1:1 minor groove complex previously reported (19) and our 2:1 complex (Figs. 3 and 4) suggests that the extremities of the hexamer are the second site of binding. This is consistent with experimental intermolecular NOEs, not attrib-

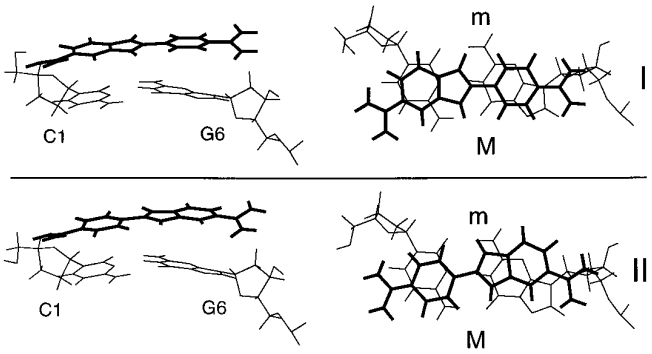

FIG. 8. **Models of the two stacking interactions (I and II) of DAPI on the outside of $(d(CGATCG))_2$, obtained after molecular mechanics and dynamics calculations.** Views looking into the major groove (*left*) and down the helix axis (*right*) show the stacking arrangement of drug with C1:G6 base aromatic rings on the outside DNA hexamer. In the view down the helix axis minor (*m*) and major (*M*) grooves are indicated.

utable to the minor groove binding, observed between DAPI protons and both minor groove and major groove protons of the last C1:G6 base pairs. Moreover, the strong upfield shift (0.55 ppm) of G6H1 imino resonance is consistent with an intercalation-like binding of the ligand involving the last C1:G6 base pair according to the observed upfield shift of drug resonances. However, the absence of any intermolecular NOE, also in long mixing time experiments, involving G2 nucleotide together with the observation that the binding does not cause an increase of internucleotide sequential distances between C1 and G2 as well as C5 and G6 residues, indicates that intercalation of ligand between the two last base pairs can be excluded. Therefore, based on intermolecular NOEs, spectral changes and DNA structure perturbations, these results are consistent with a π,π-stacking interaction of aromatic rings of DAPI with the terminal C1:G6 base pair on the outside of hexamer.

The starting structures for molecular mechanics and molecular dynamics calculations were generated by adding a DAPI molecule to the fully refined structure of minor groove complex. The ligand was manually docked and positioned to meet NOE data. Lower bound of 1.7 Å and upper bounds ranging from 3.9 to 4 Å were used in calculations for all NMR-derived intermolecular distances involving stacked complexes and not attributable to minor groove binding. In addition, all NOE-derived distance restraints used for minor groove molecular modeling were applied in restrained calculations. Since NOE data are not consistent with a single model of stacking binding, different orientations of the drug were tentatively simulated also accounting for not observed intermolecular NOEs. The results show that NOEs are consistent with fast exchange of ligand between the two different orientations (I and II) of the drug shown in the binding models of Fig. 8. No satisfactory results were obtained by simulating different orientations of the ligand. Structures I and II were obtained by using intermolecular NOE distance restraints not attributable to minor groove binding: DAPIH3′-G6H8, DAPIH4-C1H1′, DAPIH5-C1H1′, DAPIH5-C1H6, and DAPIH7-G6H8, DAPIH3′-C1H1′, DAPIH5′-C1H5, respectively. It has to be pointed out that intermolecular NOEs such as DAPIH5′-G6H1′ and DAPIH5-G6H1′, for instance, observed in long mixing time NOESY experiments (Fig. 3) and attributable to spin diffusion of minor groove complex are also compatible with the proposed model for stacking interaction (Fig. 8). In both the structures of Fig. 8 the drug is located with its positively charged amidine groups close to the phosphate backbones and NH indole proton oriented toward major groove, accounting for the observed NOEs between its H4 and H5 protons and C1H1′ as well as its H7 and G6H8 of hexamer. The orientation of the drug with respect to DNA base pairs is quite similar to that proposed for intercalation of DAPI (9) and consistent with NMR results obtained for DAPI intercalation in $(d(CGACGTCG))_2$ (20).

Conclusions—Two minor groove complexes of DAPI with DNA oligomers have been previously characterized by x-ray crystallographic analysis (13) and NMR spectroscopy (19). Effects attributable to DNA length and sequence on DAPI minor binding are evidenced by a comparative analysis of our results with those previously reported.

In the site of binding, minor groove interaction induces quite similar strong shifts of DNA resonances in the presence (this work) and in the absence (19) of stacking interaction. This indicates that position and orientation of aromatic rings of ligand in our minor groove complex is not perturbed by the second binding. However, at a 1:1 drug/duplex ratio, stacked interaction in our complex is already observable, and it is not present in the complex with octamer $(d(GCGATCGC))_2$ (19) which contains the same sequence of our hexamer $[d(CGATCG)]_2$. This suggests an effect of DNA length on the association constant of the minor groove interaction but not on the binding structure, probably attributable to the lower stability of hexamer double helix compared with octamer.

As previously reported, the minimum requirement for minor groove binding of DAPI are two contiguous A:T base pairs (19). The guanine N2 amino group of C:G base pairs, flanking the 5′-AT-3′ tract, reduces the binding constant with respect to more extended A:T regions but does not prevent the interaction (19, 20). However, owing to the restricted number of intermolecular NOEs, precise structural details about the effects of the flanking C:G base pairs on the accommodation of ligand within minor groove of only two contiguous A:T base pairs were not previously reported (19). These effects clearly appear by comparing the results of this work with the minor groove complex of DAPI within the central 5′-AATT-3′ region of $(d(CGCGAATTCGCG))_2$, previously characterized by x-ray crystallographic analysis (13). Although in both the structures NH indole proton of DAPI is positioned to form a bifurcated hydrogen bond with the two thymine O2 of the central A:T base pairs (Fig. 7), in the crystal structure the phenyl ring of the drug is inserted deeper into the minor groove by about 1.5 Å. Steric clash and electrostatic repulsion with N2 amino group of guanines, belonging to the 5′-GATC-3′ binding site of hexamer, push phenyl amidine group of ligand away from the bottom of the groove to form a hydrogen bond with O1P of G2. In contrast, indole amidine group of DAPI does not overlap with the C:G base pairs flanking the 5′-AT-3′ tract of hexamer and conserves the deep insertion into the minor groove as well as the hydrogen bond with N3 of the central adenine observed in the crystal structure. Therefore, decreased van der Waals interaction within minor groove and electrostatic repulsion involving drug phenyl ring appear responsible for the previously observed lower affinity of DAPI to the minor groove of only two contiguous A:T base pairs in comparison with more extended A:T tracts (15, 19).

Although ligand fast exchanges, on the NMR time scale, among different sites, the results clearly indicate a novel binding of DAPI by an outside π,π-stacking interaction with the terminal C1:G6 base pairs of hexamer. The absence of any increase of internucleotide sequential distances suggests that outside stacked interaction is favored in comparison with intercalation in 5′-CG-3′ site (20) by minor groove binding inside DNA hexamer.

In conclusion, although minor groove interaction in AT sites is the strongest way of binding of DAPI to double-stranded DNA, stacking interactions, also considering intercalation, is a more widespread way of binding. Stacking interactions have

been also suggested for binding of DAPI to single-stranded DNA based on upfield shift of ligand resonances (20), and intercalation is the most favorable interaction of the drug with RNA (50). For this reason, in attempting to explain the reported biological effects of DAPI, in addition to minor groove binding, stacking interactions should be considered principally when biological effects are observed at high drug-nucleotide molar ratios or target nucleic acid is not double-stranded DNA.

Acknowledgments—We thank Dr. Daniela Orrú for helpful discussion and Fabio Bertocchi and Enrico Rossi for technical assistance with 400 and 600 MHz instruments. The NMR Service of the CNR Research Area of Montelibretti, Roma, courtesy of A. L. Segre, is gratefully acknowledged for running the 600 MHz experiments.

REFERENCES

1. Storl, K., Storl, J., Zimmer, C. H., and Lown, J. W. (1993) *FEBS Lett.* **317,** 157–162
2. Palù, G., Valisena, S., Barcellona, M. L., Masotti, L., and Meloni, G. A. (1987) *Biochem. Biophys. Res. Commun.* **145,** 40–45
3. Parolin, C., Zanotti, G., and Palù, G. (1995) *Biochem. Biophys. Res. Commun.* **208,** 332–338
4. Welch, J. J., Rauscher, F. J., III, and Beerman, T. A. (1994) *J. Biol. Chem.* **269,** 31051–31058
5. Parolin, C., Montecucco, A., Chiarocchi, G., Pedrali-Noy, G., Valisena, S., Palumbo, M., and Palù, G. (1990) *FEMS Microbiol. Lett.* **68,** 341–346
6. Straney, D. C., and Crothers, D. M. (1987) *Biochemistry* **26,** 1987–1995
7. Chiang, S.-Y., Welch, J., Rausher, F. J., III, and Beerman, T. A. (1994) *Biochemistry* **33,** 7033–7040
8. Wilson, W. D., Tanious, F. A., Barton, H. J., Jones, R. L., Fox, K., Wydra, R. L., and Strekowski, L. (1990) *Biochemistry* **29,** 8452–8461
9. Wilson, W. D., Tanious, F. A., Barton, H. J., Wydra, R. L., Jones, R. L., Boykin, D. W., and Strekowski, L. (1990) *Anti-Cancer Drug Des.* **5,** 31–42
10. Wilson, W. D., Tanious, F. A., Barton, H. J., Strekowski, L., and Boykin, D. W. (1989) *J. Am. Chem. Soc.* **111,** 5008–5010
11. Kubista, M., Åkerman, B., and Nordén, B. (1987) *Biochemistry* **26,** 4545–4553
12. Manzini, G., Barcellona, M. L., Avitabile, M., and Quadrifoglio, M. (1983) *Nucleic Acids Res.* **11,** 8861–8876
13. Larsen, T. A., Goodsell, D. S., Cascio, D., Grzeskowiak, K., and Dickerson, R. E. (1989) *J. Biomol. Struct. & Dyn.* **7,** 477–491
14. Loontiens, F. G., McLaughlin, L. W., Diekmann, S., and Clegg, R. M. (1991) *Biochemistry* **30,** 182–189
15. Jansen, K., Nordén, B., and Kubista, M. (1993) *J. Am. Chem. Soc.* **115,** 10527–10530
16. Kim, S. K., Eriksson, S., Kubista, M., and Nordén, B. (1993) *J. Am. Chem. Soc.* **115,** 3441–3447
17. Sehlstedt, U., Kim, S. K., and Nordén, B. (1993) *J. Am. Chem. Soc.* **115,** 12258–12263
18. Mohan, S., and Yathindra, N. (1994) *J. Biomol. Struct. & Dyn.* **11,** 849–867
19. Trotta, E., D'Ambrosio, E., Del Grosso, N., Ravagnan, G., Cirilli, M., and Paci, M. (1993) *J. Biol. Chem.* **268,** 3944–3951
20. Trotta, E., D'Ambrosio, E., Ravagnan, G., and Paci, M. (1995) *Nucleic Acids Res.* **23,** 1333–1340
21. Eriksson, S., Kim, S. K., Kubista, M., and Nordén, B. (1993) *Biochemistry* **32,** 2987–2998
22. Kapuscinski, J., and Szer, W. (1979) *Nucleic Acids Res.* **6,** 3519–3534
23. Tanious, F. A., Spychala, J., Kumar, A., Greene, K., Boykin, D. W., and Wilson, W. D. (1994) *J. Biomol. Struct. & Dyn.* **11,** 1063–1083
24. Samuelson, P., Jansen, K., and Kubista, M. (1994) *J. Mol. Recognit.* **7,** 233–241
25. Kastrup, R. V., Young, M. A., and Krugh, T. R. (1978) *Biochemistry* **17,** 4855–4865
26. Kapuscinski, J., and Skoczylas, B. (1977) *Anal. Biochem.* **83,** 252–257
27. Rance, M., Sørensen, O. W., Bodenhausen, G., Wagner, G., Ernst, R. R., and Wüthrich, K. (1983) *Biochem. Biophys. Res. Commun.* **117,** 479–485
28. Mueller, L. (1987) *J. Magn. Reson.* **72,** 191–196
29. Bax, A., and Davis, D. G. (1986) *J. Magn. Reson.* **65,** 355–360
30. Braunschweiler, L., and Ernst, R. R. (1983) *J. Magn. Reson.* **53,** 521–528
31. Jeener, J., Meier, B. H., Bachmann, P., and Ernst, R. R. (1979) *J. Chem. Phys.* **71,** 4546–4553
32. Marion, D., and Wutrich, K. (1983) *Biochem. Biophys. Res. Commun.* **113,** 967–974
33. Sklenar, V., and Bax, A. (1987) *J. Magn. Reson.* **74,** 469–479
34. Boelens, R., and Vuister, G. (1990) *Software for Processing Multidimensional NMR Spectra*, version 3/21/90, Utrecht, The Netherlands
35. Conte, M. R., Jenkins, T. C., and Lane, A. N. (1995) *Eur. J. Biochem.* **229,** 443–444
36. Clore, G. M., and Gronenborn, A. M. (1985) *FEBS Lett.* **179,** 187–192
37. Hare, D. R., Wemmer, D. E., Chou, S. H., Drobny, G., and Reid, B. R. (1983) *J. Mol. Biol.* **171,** 319–336
38. Hosur, R. V., Ravikumar, M., Roy, K. B., Zu-Kun, T., Miles, H. T., and Govil, G. (1985) in *Magnetic Resonance in Biology and Medicine* (Govil, G., Khetrapal, C. L., and Saran, A., eds) pp. 243–260, Tata McGraw-Hill, New Delhi
39. Reid, D. G., Salisbury, S. A., Bellard, S., Shakked, Z., and Williams, D. H. (1983) *Biochemistry* **22,** 2019–2025
40. Scheek, R. M., Russo, N., Boelens, R., Kaptein, R., and van Boom, J. H. (1983) *J. Am. Chem. Soc.* **105,** 2914–2916
41. Scheek, R. M., Boelens, R., Russo, N., van Boom, J. H., and Kaptein, R. (1984) *Biochemistry* **23,** 1371–1376
42. Boelens, R., Sheek, R. M., Dijkstra, K., and Kaptein, R. (1985) *J. Magn. Reson.* **62,** 378–386
43. Wüthrich K. (1986) *NMR of Proteins and Nucleic Acids*, pp. 203–255, John Wiley & Sons, Inc., New York
44. Patel, D. J., Shapiro, L., and Hare, D. (1987) *Q. Rev. Biophys.* **20,** 35–112
45. Hosur, R. V., Govil, G., and Miles, H. T. (1988) *Magn. Reson. Chem.* **26,** 927–944
46. Davies, D. B. (1978) *Prog. Nucl. Magn. Reson. Spectrosc.* **12,** 135–225
47. Altona, C. (1982) *Recl. Trav. Chim. Pays-Bas. Belg.* **101,** 413–433
48. Lown, J. W., Hanstock, C. C., Bleackley, R. C., Imbach, J. L., Rayner, B., and Vasseur, J. J. (1984) *Nucleic Acids Res.* **12,** 2519–2533
49. Feigon, J., Denny, W. A., Leupin, W., and Kearns, D. R. (1984) *J. Med. Chem.* **27,** 450–465
50. Tanious, F. A., Veal, J. M., Buczak, H., Ratmeyer, L. S., and Wilson, W. D. (1992) *Biochemistry* **31,** 3103–3122

Simultaneous and Different Binding Mechanisms of 4′,6-Diamidino-2-phenylindole to DNA Hexamer (d(CGATCG))$_2$: A 1H NMR STUDY

Edoardo Trotta, Ettore D'Ambrosio, Giampietro Ravagnan and Maurizio Paci

J. Biol. Chem. 1996, 271:27608-27614.
doi: 10.1074/jbc.271.44.27608